

Supplementary information

September 7, 2020

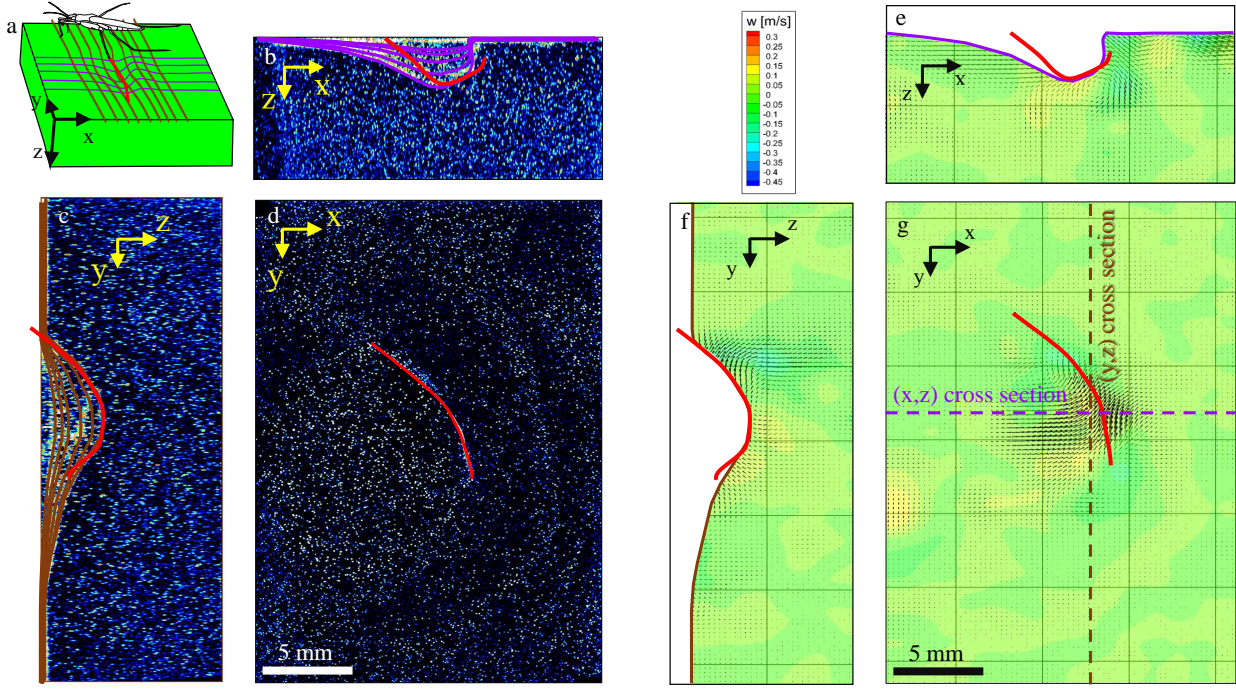


Figure S1: Multiple projections of the reconstructed volume of particles during the (forward) sculling of a water strider. This figure is a snapshot taken 15 ms after the start of a leg stroke. (a) The images taken by a camera, placed above the water tank, allow us to estimate the exact location of the water strider body and legs in the tomoPIV measurement domain. We used the images of that camera to produce this sketch, which illustrates the relative location of the tomoPIV domain (green volume) and insect body. We also superimposed different sections of the surface topography using the same color code than in (b) and (c). (b) Projection in (z,x) plane. The magenta curves illustrate the estimated location of the air-water interface. As it is a projection, we have superimposed the different estimates of the surface position for different y values. (c) Projection in (z,y) plane. The brown curves illustrate the estimated position of the air-water interface. (d) Projection in the (x,y) plane. The red curve corresponds to the estimated position of the leg instantaneous location at 15 ms. (e) Cross section in the (z,y) plane of the 3D velocity field. The section position is represented in (g) in dotted line. (f) Cross section in the (z,x) plane of the 3D velocity field. The section position is represented in (g) in dotted line. (g) Cross section in the (x,y) plane of the 3D velocity field obtained after cross correlation of the voxel spaces.

Parameters	Expression (Units)	Numerical value
Diffuse interface thickness	ϵ (m)	80×10^{-6}
Free mixing energy	λ (N)	6×10^{-6}
Mobility tuning parameter	χ (m.s/kg)	5
Mobility	$\gamma = \chi \epsilon^2$ (m ³ .s/kg)	16×10^{-9}
Surface tension	σ (N/m)	72×10^{-3}
Cylinder contact angle	θ_w (rad)	$\pi/8$
Air density	ρ_{air} (kg/m ³)	1.2
Air viscosity	μ_{air} (Pa.s)	1.78×10^{-5}
Water density	ρ_{water} (kg/m ³)	1000
Water viscosity	μ_{water} (Pa.s)	8.9×10^{-4}
Gravitational acceleration	g (m/s ²)	9.81
Capillary length	$l_c = \sqrt{\frac{\sigma}{\rho_{water}g}}$ (m)	2.7×10^{-3}
Cylinder diameter	D_{cyl} (m)	200×10^{-6}
Horizontal leg velocity	U_{leg} (m/s)	0.2 – 0.7
Vertical leg velocity	V_{leg} (m/s)	0
Depth of stroke	h_d (m)	$0.6 \times 10^{-3} - 3 \times 10^{-3}$
Ohnesorge number	$Oh = \frac{\mu_{water}}{\sqrt{\rho_{water}\sigma}l_c}$	2.0×10^{-3}
Weber number	$We = \frac{\rho_{water}(U_{leg}^2 + V_{leg}^2)l_c}{\sigma}$	1.5 – 18.4
Cahn number	$Cn = \frac{\epsilon}{l_c}$	7.4×10^{-3}

Table S1. Expressions and numerical value of the parameters governing the physical problem. The Ohnesorge (Oh) , Weber (We) and Cahn (Ca) number measure, respectively, the strength of viscous force with respect to the inertial force and the interfacial tension, the dimensionless interfacial thickness and the relative importance of inertia to interfacial tension.

Experiments on mechanical leg $d=100\ \mu\text{m}$

Numerical simulation $d=200\ \mu\text{m}$

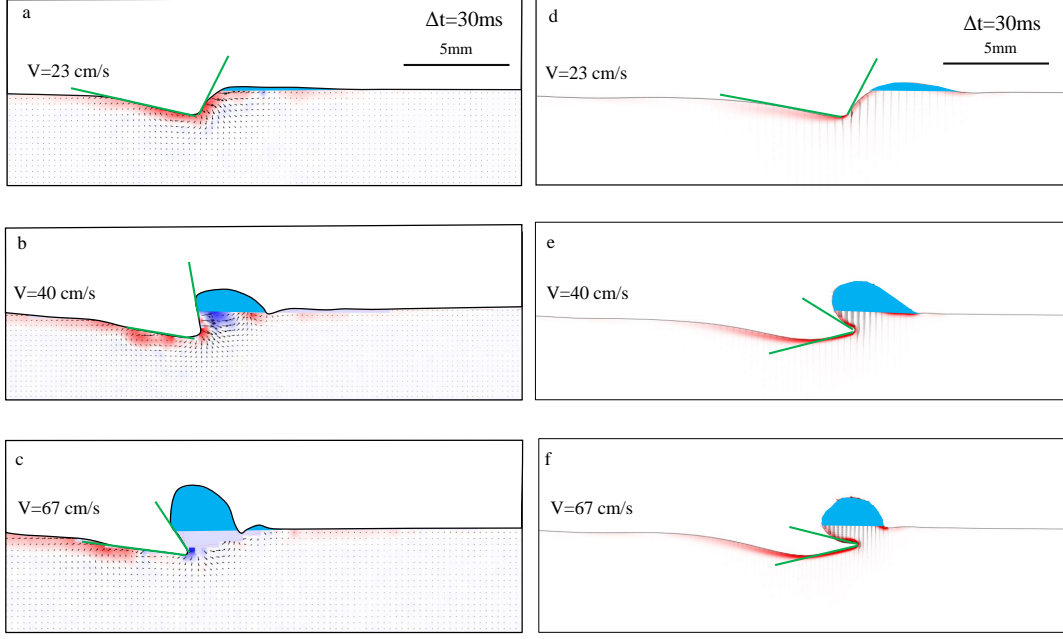


Figure S2: Comparison between experiments and numerical simulations. Influence of the velocity of stroke V_l on forces and momentum contributions at fixed depth $h_l=0.95\ \text{mm}$. We estimated, for each measurement, the bow wave momentum p_{bw} , the time integral of surface tension forces p_s and the fluid momentum p_f . The estimation and comparison is done at $\Delta t=30\ \text{ms}$ after the start of translation. (Left Column) Experiments on mechanical leg, $d=100\ \mu\text{m}$. (a) Leg velocity $V_l=23\ \text{cm/s}$, $p_{bw}=2.8 \times 10^{-4}\ \text{kg/s}$, $p_s=7.3 \times 10^{-4}\ \text{kg/s}$ (with $\alpha_a=11\ \text{deg}$ and $\alpha_p=50\ \text{deg}$) and $p_f=5.5 \times 10^{-4}\ \text{kg/s}$. (b) Leg velocity $V_l=40\ \text{cm/s}$, $p_{bw}=1 \times 10^{-3}\ \text{kg/s}$, $p_s=2 \times 10^{-3}\ \text{kg/s}$ (with $\alpha_a=0\ \text{deg}$ and $\alpha_p=90\ \text{deg}$) and $p_f=6.4 \times 10^{-4}\ \text{kg/s}$. (c) Leg velocity $V_l=67\ \text{cm/s}$, $p_{bw}=2.3 \times 10^{-3}\ \text{kg/s}$, $p_s=3 \times 10^{-3}\ \text{kg/s}$ (with $\alpha_a=0\ \text{deg}$ and $\alpha_p=120\ \text{deg}$) and $p_f=6.3 \times 10^{-4}\ \text{kg/s}$. (Right Column) Numerical simulations, $d=200\ \mu\text{m}$. (d) Leg velocity $V_l=23\ \text{cm/s}$, $p_{bw}=6.9 \times 10^{-4}\ \text{kg/s}$, $p_s=7.3 \times 10^{-4}\ \text{kg/s}$ (with $\alpha_a=11\ \text{deg}$ and $\alpha_p=50\ \text{deg}$) and $p_f=5.1 \times 10^{-4}\ \text{kg/s}$. (e) Leg velocity $V_l=40\ \text{cm/s}$, $p_{bw}=2.7 \times 10^{-3}\ \text{kg/s}$, $p_s=3.9 \times 10^{-3}\ \text{kg/s}$ (with $\alpha_a=-16\ \text{deg}$ and $\alpha_p=150\ \text{deg}$) and $p_f=9.8 \times 10^{-4}\ \text{kg/s}$. (f) Leg velocity $V_l=67\ \text{cm/s}$, $p_{bw}=3.6 \times 10^{-3}\ \text{kg/s}$, $p_s=4.2 \times 10^{-3}\ \text{kg/s}$ (with $\alpha_a=-14\ \text{deg}$ and $\alpha_p=166\ \text{deg}$) and $p_f=6.6 \times 10^{-4}\ \text{kg/s}$.

Experiments on mechanical leg $d=100\ \mu\text{m}$

Numerical simulation $d=200\ \mu\text{m}$

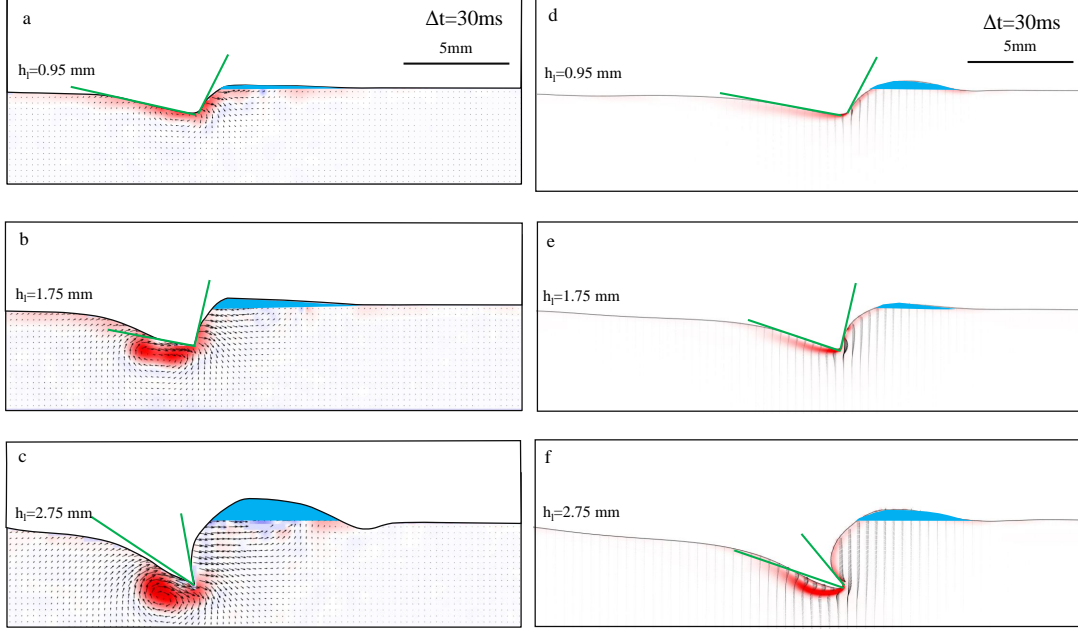


Figure S3: Comparison between experiments and numerical simulations. Influence of depth of stroke on forces and momentum contributions at fixed velocity $V=0.23\ \text{m/s}$. We estimated, for each measurement, the bow wave momentum p_{bw} , the time integral of surface tension forces p_s and the fluid momentum p_f . The estimation and comparison is done at $\Delta t=30\ \text{ms}$ after the start of translation. (Left Column) Experiments on mechanical leg, $d=100\ \mu\text{m}$. (a) Leg velocity $V_l=23\ \text{cm/s}$, $p_{bw}=2.8 \times 10^{-4}\ \text{kg/s}$, $p_s=7.3 \times 10^{-4}\ \text{kg/s}$ (with $\alpha_a=11\ \text{deg}$ and $\alpha_p=50\ \text{deg}$) and $p_f=5.5 \times 10^{-4}\ \text{kg/s}$. (b) Leg depth $h_l=1.75\ \text{mm}$, $p_{bw}=3.3 \times 10^{-4}\ \text{kg/s}$, $p_s=1.3 \times 10^{-3}\ \text{kg/s}$ (with $\alpha_a=15\ \text{deg}$ and $\alpha_p=71\ \text{deg}$) and $p_f=1.6 \times 10^{-3}\ \text{kg/s}$. (c) Leg depth $h_l=2.75\ \text{mm}$, $p_{bw}=9.4 \times 10^{-4}\ \text{kg/s}$, $p_s=2.3 \times 10^{-3}\ \text{kg/s}$ (with $\alpha_a=22\ \text{deg}$ and $\alpha_p=100\ \text{deg}$) and $p_f=2.3 \times 10^{-3}\ \text{kg/s}$. (Right Column) Numerical simulations, $d=200\ \mu\text{m}$. (d) Leg velocity $V_l=23\ \text{cm/s}$, $p_{bw}=6.9 \times 10^{-4}\ \text{kg/s}$, $p_s=7.3 \times 10^{-4}\ \text{kg/s}$ (with $\alpha_a=11\ \text{deg}$ and $\alpha_p=50\ \text{deg}$) and $p_f=5.1 \times 10^{-4}\ \text{kg/s}$. (e) Leg depth $h_l=1.75\ \text{mm}$, $p_{bw}=2.3 \times 10^{-5}\ \text{kg/s}$, $p_s=1.5 \times 10^{-3}\ \text{kg/s}$ (with $\alpha_a=18\ \text{deg}$ and $\alpha_p=76\ \text{deg}$) and $p_f=8.5 \times 10^{-4}\ \text{kg/s}$. (f) Leg depth $h_l=2.75\ \text{mm}$, $p_{bw}=6 \times 10^{-4}\ \text{kg/s}$, $p_s=3.4 \times 10^{-3}\ \text{kg/s}$ (with $\alpha_a=17.6\ \text{deg}$ and $\alpha_p=130\ \text{deg}$) and $p_f=1.7 \times 10^{-3}\ \text{kg/s}$.

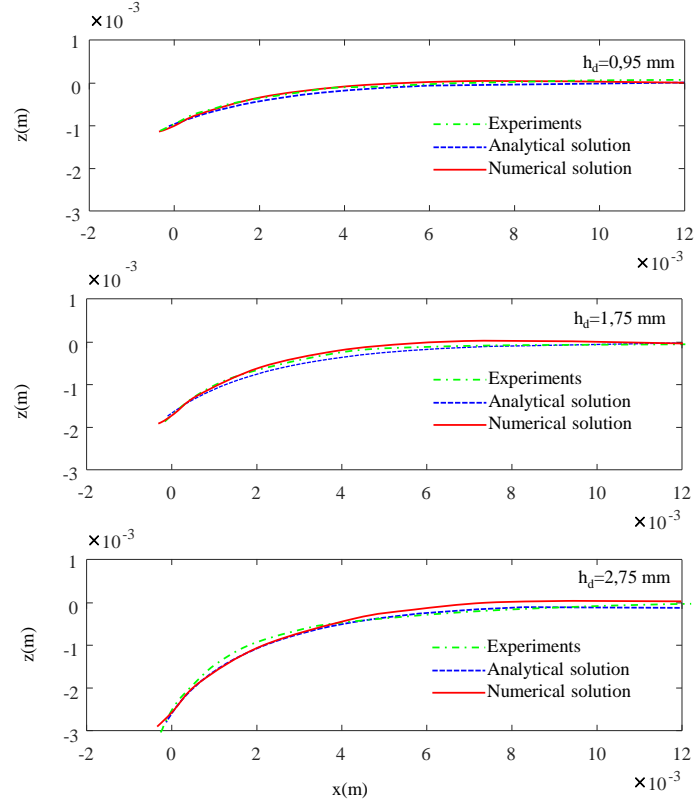


Figure S4: Static comparison between numerical model, analytical solution of meniscus profile using the analytical solution of DeGennes et al (2004) and experiment for varying depth of leg penetration.

D. de Gennes, Pierre-Gilles, Brochard-Wyart, Françoise, Quéré. Capillarity and Wetting Phenomena. Springer, 2004.

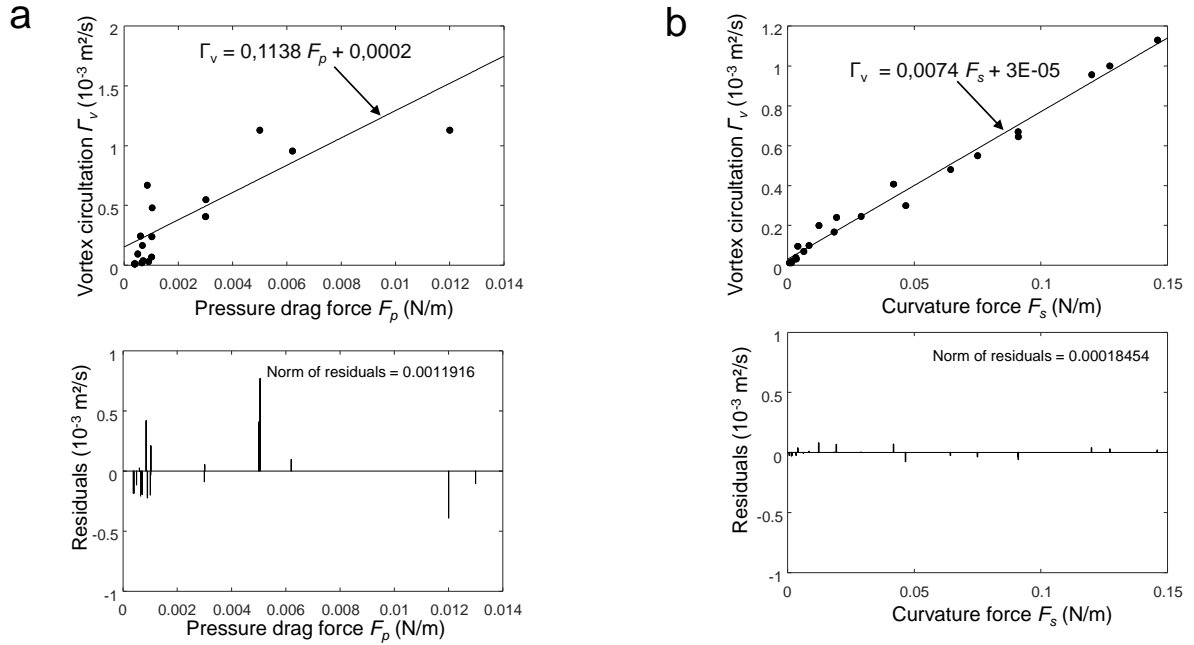


Figure S5: Evolution of vortex circulation with propulsive forces. This figure is produced on the basis of the analysis of the vortex circulation derived from numerical simulations of interface and fluid bulk for sculling legs.